Journal of Hazardous Materials 442 (2023) 130057

Contents lists available at ScienceDirect

Journal of Hazardous Materials

journal homepage: www.elsevier.com/locate/jhazmat

Research Paper

Microbial communities mediating net methylmercury formation along a trophic gradient in a peatland chronosequence

Baolin Wang [a,b], Haiyan Hu [a,*], Kevin Bishop [b], Moritz Buck [b], Erik Björn [c], Ulf Skyllberg [d], Mats B. Nilsson [d], Stefan Bertilsson [b], Andrea G. Bravo [e]

[a] State Key Laboratory of Environmental Geochemistry, Institute of Geochemistry, Chinese Academy of Sciences, 550081 Guiyang, China
[b] Department of Aquatic Sciences and Assessment, Swedish University of Agricultural Sciences, SE-75007 Uppsala, Sweden
[c] Department of Chemistry, Umeå University, SE-90187 Umeå, Sweden
[d] Department of Forest Ecology and Management, Swedish University of Agricultural Sciences, SE-90183 Umeå, Sweden
[e] Department of Marine Biology and Oceanography, Institut de Ciències del Mar (ICM-CSIC), Pg Marítim de la Barceloneta 37–49, E08003 Barcelona, Catalunya, Spain

HIGHLIGHTS

- Microbial community composition clearly differed along the peatland chronosequence.
- Net MeHg formation was linked to composition and activity of microbial communities.
- Fermenters, syntrophs, and methanogens correlated positively with MeHg formation.
- Sulfate reducers may be less prominent in MeHg formation than previously thought.

GRAPHICAL ABSTRACT

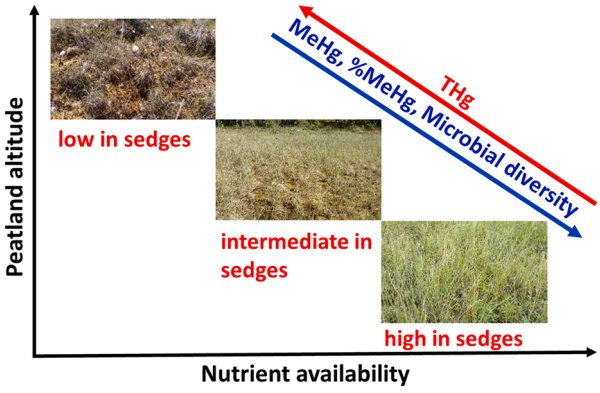

ARTICLE INFO

Editor: Jörg Rinklebe

Keywords:
Microbial Community
Mercury
MeHg
Mercury methylation
Peatland trophic gradient

ABSTRACT

Peatlands are generally important sources of methylmercury (MeHg) to adjacent aquatic ecosystems, increasing the risk of human and wildlife exposure to this highly toxic compound. While microorganisms play important roles in mercury (Hg) geochemical cycles where they directly and indirectly affect MeHg formation in peatlands, potential linkages between net MeHg formation and microbial communities involving these microorganisms remain unclear. To address this gap, microbial community composition and specific marker gene transcripts were investigated along a trophic gradient in a geographically constrained peatland chronosequence. Our results showed a clear spatial pattern in microbial community composition along the gradient that was highly driven by peat soil properties and significantly associated with net MeHg formation as approximated by MeHg concentration and %MeHg of total Hg concentration. Known fermentative, syntrophic, methanogenic and iron-reducing metabolic guilds had the strong positive correlations to net MeHg formation, while methanotrophic and methylotrophic microorganisms were negatively correlated. Our results indicated that sulfate reducers did not have a

* Corresponding author.
E-mail address: huhaiyan@mail.gyig.ac.cn (H. Hu).

https://doi.org/10.1016/j.jhazmat.2022.130057
Received 3 July 2022; Received in revised form 5 September 2022; Accepted 19 September 2022
Available online 23 September 2022

key role in net MeHg formation. Microbial activity as interpreted from 16S rRNA sequences was significantly correlated with MeHg and %MeHg. Our findings shed new light on the role of microbial community in net MeHg formation of peatlands that undergo ontogenetic change.

1. Introduction

Mercury (Hg) has long been known as a global environmental contaminant due to its potential for long-distance transport. One of its chemical species, methylmercury (MeHg), is of particular concern because of its tendency to bioaccumulate in aquatic and terrestrial food webs in combination with its high toxicity to wildlife and humans (Clarkson and Magos, 2006; Feng et al., 2008; Hong et al., 2012; Meng et al., 2011; Zhang et al., 2010a, 2010b). Various studies have demonstrated a crucial role for peatlands in Hg cycling since they are typically exporting MeHg to adjacent aquatic ecosystems while they are generally sinks for total Hg (THg) (Mitchell et al., 2008; St. Louis et al., 1996; Tjerngren et al., 2012). Therefore, a greater understanding of MeHg formation within such peatland ecosystems is critical for devising effective land management strategies that limit MeHg production and constrain health risks related to Hg (Bergman et al., 2012; Bishop et al., 2020).

Transformation from inorganic Hg (IHg) to MeHg is mediated by anaerobic microorganisms that host the *hgcAB* genes (Parks et al., 2013). These genes are found in sulfate-reducing bacteria (SRB) (Compeau and Bartha, 1985; Gilmour et al., 1992, 2013), iron-reducing bacteria (FeRB) (Bravo et al., 2018b; Fleming et al., 2006; Kerin et al., 2006), and methanogens (Hamelin et al., 2011; Wood et al., 1968), but also in some fermentative and syntrophic microbes (Gilmour et al., 2013; Podar et al., 2015; Yu et al., 2018). Recently the wider use of culture-independent methods, such as *hgcA* gene sequencing, genome-resolved metagenomics and metatranscriptomics, has greatly expanded the known phylogenetic and metabolic diversity of Hg methylating microorganisms (Christensen et al., 2019; McDaniel et al., 2020; Peterson et al., 2020; Xu et al., 2019, 2021). While FeRB, methanogens, syntrophs and Firmicutes have been implicated as putative Hg methylating microorganisms in low-sulfate wetlands, SRB remain the main methylators in the ecosystems where sulfate is not limiting (Liu et al., 2018; Roth et al., 2021; Schaefer et al., 2020; Xu et al., 2021).

Nevertheless, the actual formation of MeHg appears to be only weakly related to the presence or expression of Hg methylating genes (Bouchet et al., 2018; Bravo et al., 2016; Christensen et al., 2019; Paranjape and Hall, 2017; Xu et al., 2021). Additionally, recent studies have recognized the hitherto underappreciated role of non-Hg methylating microorganisms as influencing net MeHg formation (Liu et al., 2019; Xu et al., 2019). The non-methylating microbes can mediate other Hg transformation processes such as demethylation, reduction, oxidation and sequestration (Barkay and Gu, 2022; Barkay and Wagner-Döbler, 2005; Grégoire and Poulain, 2018) but also maintain complex metabolic interactions with the Hg methylating lineages (Bravo et al., 2018a; Correia et al., 2012). Clearly, net MeHg formation is not only dependent on Hg methylating microbes but the entire communities where Hg methylators are embedded. Therefore, we need to reach a better understanding of how the composition of microbial communities, including both Hg and non-Hg methylating microbes, influence net MeHg formation.

Numerous studies have found that microbial community composition and abundance are highly sensitive to the heterogeneous environmental conditions in peatlands, such as pH, redox potential, nutrient availability and vegetation (Bragazza et al., 2015; Fisk et al., 2003; Morales et al., 2006; Urbanová and Bárta, 2014). Such factors can be studied in manipulation experiments in either the field or the laboratory (Åkerblom et al., 2020; Haynes et al., 2017). However, the short-term nature of most such manipulations may introduce artifacts that complicate interpretation. Natural chronosequence ecosystems can be used as a form of long-term manipulation where isostatic rebound of land areas after the last glaciation has led to the formation of peatland ecosystems with dramatically different ages within geographically constrained areas. Examples of such chronosequences can be found on the coastline around the Gulf of Bothnia between Finland and Sweden, an area which is still rising at a rate of about 8.5 mm/year (Hünicke et al., 2015). Along chronosequences, the connection of peat at the top of the soil profiles with the underlying mineral substrates decreases over time as the peat builds up. This is paralleled by a depletion in the peat of dissolved minerals and other weathering products originating from either those mineral substrates or imports from the watersheds surrounding the peatlands (Wang et al., 2020). A peatland chronosequence therefore creates a wide range of contrasting vegetation, hydrology and nutrient availability within a limited geographic area (10–20 km). This provides a natural trophic gradient for evaluating long-term biogeochemical effects on microbial community composition and subsequent net MeHg formation.

Across the peatland chronosequence within a few kilometers of the coast of the Baltic Sea's Bothnian Bay in northern Scandinavia, there is a trophic gradient in peatlands that experience similar atmospheric deposition and climate patterns and also share a similar underlying geology. Our previous studies on this chronosequence have linked the characteristics (i.e. nutrients and other geochemical parameters) of fifteen peatlands divided into three age classes (i.e. young, intermediate and old peatlands) to gradual changes in concentrations of THg and MeHg in solid peat, with higher MeHg but lower THg observed in the nutrient-rich younger peatlands (Wang et al., 2020). The apparently higher net MeHg formation in younger peatlands was attributed to the higher availability of organic matter and appropriate electron acceptors as well as the higher IHg solubility enhanced by the formation of Hg-polysulfide compounds in the younger peatlands (Wang et al., 2021). We also investigated whether vascular plant removal would impact Hg methylation within peatlands along the chronosequence by reducing the availability of readily available organic matter (i.e. root exudates). Surprisingly, this had no discernible effect on Hg methylation. Moreover, the peat soils collected from three peatlands representing three age classes have also been analyzed for the contribution of different microbial processes (e.g. sulfate reduction, iron reduction, methanogenesis and fermentation) to Hg methylation by means of specific inhibitor/-stimulator amendment incubations (Hu et al., 2020).

This current study builds on these previously published studies with the primary goal of relating microbial community composition to net MeHg formation along the peatland chronosequence. This is done by (1) mapping the composition of microbial communities, (2) assessing the putative functional role of key microbial taxa in net MeHg formation, and (3) determining the activity of specific functional microbial groups. We used high-throughput Illumina sequencing of 16S rRNA gene amplicons and quantitative PCR for protein coding marker genes to describe the composition of microbial communities and the abundance of specific functional groups as well as to establish associations between microbial communities and net MeHg formation.

2. Materials and methods

2.1. Site description, sampling and sample preparation

A chronosequence of 15 open peatlands along the Gulf of Bothnia in northern Sweden was sampled during 2016 and 2017 (Fig. S1 in the Supplementary Information (SI)). More detailed information on the site, clean sampling and sample preparation is given elsewhere (Wang et al.,

2020, 2021). Briefly, the chronosequence features a natural gradient of trophic status and hydrogeochemistry with respect to vegetation composition and other geochemical and geomorphological features. The 15 peatlands selected from the chronosequence were evenly divided into three age groups, young (< 1000 years, n = 5), intermediate (1000 ~ 2000 years, n = 5) and old (> 2000 years, n = 5). Notably, the age of superficial peat is expected to be similar, regardless of the time since peatlands started to form.

Five 70 × 210 cm plots were established within each of the fifteen peatlands in June 2016, with each plot divided into three 70 × 70 cm subplots: one control subplot, one treatment subplot (complete vascular plant removal, VPR) as well as one buffer subplot between these other two. The VPR treatment is supposed to reduce the availability of readily available organic matter (e.g. root exudates) to methylating microorganisms and consequently to influence Hg methylation. Peat samples were sampled four times from both the control and VPR subplots in June (the beginning of the growing season) and August (growing season) during 2016 and 2017, with one exception from the VPR subplots in June 2016 when the VPR subplots had just been set up. A 10 × 10 × 10 cm peat core, taken immediately below the average growing season ground water table (GWT), was extracted from each subplot and cut into an upper and a lower layer (0–5 and 5–10 cm, respectively). Peat soils used for DNA (taken from all samples, 210 samples in total) and RNA extractions (taken only from 2017 samples, 60 samples in total) were randomly retrieved from different parts of the two layers using a clean pair of tweezers and kept in individual 2 ml sterile cryo microtubes. The peat samples were immediately frozen and kept in liquid nitrogen during transport and subsequently stored at − 80 °C until further processing and analysis. Peat subsamples were also taken for chemical analyses, such as MeHg, THg, total concentrations of C, S, and Fe.

2.2. Chemical analysis

The concentration of THg was measured with solid combustion atomic absorption spectrometry (DMA-80, Milestone, Italy) using the certified marine sediment reference material MESS-3 (National Research Council of Canada, 0.091 ± 0.009 mg Hg/kg) for calibration. The concentration of MeHg in peat soils was determined according to the method of Lambertsson et al. (2001). The concentration of IHg was calculated by subtracting MeHg from THg. The percentage of MeHg to THg (%MeHg) in the peat soil was also calculated. MeHg concentration and %MeHg in peat soil were used as proxies for net MeHg formation, due to its positive relationships across a wide range of different types of freshwater sediments (Drott et al., 2008). For the peat soils collected in 2016, the total concentrations of C and N were measured with an elemental analyzer (Flash EA 2000, Thermo Fisher Scientific, Bremen, Germany) and total concentrations of Ca, Fe, Mg, Mn, Na, K, Al, Zn, Si, S and P were measured using an ICP-OES (Spectro Ciros Vision, Spectro Analytical Instruments Inc., Germany). Replicate samples were routinely analyzed for all the measurements in this study. The accuracy (defined as measured divided by certified concentrations) was 95 ± 5 and 105 ± 8% for MESS-3 and ERM-CC580, respectively, while the precision was within 10% relative standard deviation.

2.3. DNA extraction and barcoded PCR amplification of 16S rRNA genes

The five upper and the five lower replicate samples were homogenized into two samples for each peatland, one upper and one lower. Approximately 0.25 g of each homogenized soil sample was used for the extraction of genomic DNA with the DNeasy PowerSoil Kit (QIAGEN Inc., Germany) according to the manufacturer's instructions. The quality of the extracted DNA was determined by gel electrophoresis (1% agarose). The V3–V4 region of the 16S rRNA gene was subsequently amplified with the primer pair, 341F (5′-CCTACGGGNGGCWGCAG-3′) − 805R (5′-GACTACNVGGGTATCTAATCC-3′), according to a two-step PCR protocol where sample-specific molecular barcodes (Table S1) were added in the second step (Sinclair et al., 2015), with slight modifications of reaction reagents and thermal programs (Table S2 and Table S3). The amplicons from the second-stage PCR were purified using magnetic beads (AMPure XP, Beckman Coulter Life Sciences, United States) and quantified using a fluorescence-based DNA quantification kit (PicoGreen, Invitrogen). Based on the quantification, the amplicons from the second-stage PCR were pooled in equal proportions to obtain a similar number of sequencing reads for each sample, followed by a final purification with the Qiagen Gel Extraction Kit (Qiagen, Germany) and quantification with the fluorescence-based DNA quantitation kit (PicoGreen, Invitrogen). The pooled amplicons were sequenced on the Illumina MiSeq platform using 2 × 300 bp paired-end approach at the SNP/SEQ SciLifeLab facility hosted by Uppsala University (https://snpseq.medsci.uu.se) where the TruSeq Sample Preparation Kit V2 was used according to the manufacturer's instructions.

2.4. Sequence Processing

Illumina reads were demultiplexed with an in-house script and then merged with USEARCH (v10) (Edgar, 2010) and quality screened ("-fastq_minlen 400 -fastq_maxee 2″, parameters) and dereplicated with singletons removed using VSEARCH (v2.7.1, an unlimited version of USEARCH) (Rognes et al., 2016). The sequences of individual samples range from 1349 to 42808 reads, with 2821853 reads in total for all the 210 samples. High-quality sequences were clustered into Operational Taxonomic Units (OTUs) at 97% identity. Chimeric sequences were removed using USEARCH's -cluster_otus method (Edgar, 2016), while taxonomy was predicted with the -sintax method using the rdp_16s_v16 database (Cole et al., 2013), provided here: https://drive5.com/usearch/manual/sintax_downloads.html. To enable the comparison between samples, sequences were rarefied to match the sample with the least number of reads. The sequences have been deposited in ENA under accession number PRJNA843367.

2.5. RNA extraction, cDNA synthesis and quantitative PCR

The peat samples collected from the five replicate plots in each peatland (the five upper layer and the five lower layer samples) on the same sampling occasion in 2017 were homogenized into an individual sample. This resulted in 60 samples in total, with two June and two August samples (one control and one VPR sample) for each of the 15 peatlands along the chronosequence. Approximately 1 g of the homogenized peat soil was used for the extraction of total soil RNA with the RNeasy PowerSoil Total RNA Kit (QIAGEN Inc., Germany) according to the manufacturer's instructions. After determining the concentration using a NanoDrop 2000 spectrophotometer (Thermo Fisher Scientific, USA), the extracted RNA was purified with a TURBO DNA-free™ Kit (AM1907, AMBIO, Life technologies, USA). The absence of DNA contamination in the RNA samples was confirmed by PCR amplification using RNA as a template. The purified RNA was then used for synthesizing complementary DNA (cDNA) with the SuperScript™ III First-Strand Synthesis System (Invitrogen, Thermo Fisher Scientific) according to the manufacturer's instructions. The RNA and cDNA samples were stored at − 80 °C until further processing and analysis.

The expression of specific marker genes (Table S4), including 16S rRNA (targeting actively growing microorganisms), *dsrA* (SRB), *mcrA* (methanogens), Archaea-*hgcA* (archaeal methylators), Deltaproteobacteria-*hgcA* (Deltaproteobacteria methylators) and SRB-firmicutes-*hgcA* (sulfate-reducing Firmicutes methylators), were quantified with real time quantitative PCR (qPCR). The qPCR was performed in 10 μL reaction volumes with a Bio-Rad CFX96 touch real-time PCR detection system using the commercial enzyme kit TATAA SYBR® GrandMaster® Mix (TATAA Biocenter AB, Sweden), according to the manufacturer's recommendations. Genomic DNAs (gDNAs) used as standards were derived from pure cultures ordered from DSMZ (Deutsche Sammlung von Mikroorganismen und Zellkulturen, https://www.dsmz.de). The

gDNA was quantified and serially diluted. The 60 cDNA samples were used as templates and the qPCR specificity was further verified by gel electrophoresis (2% agarose) after GelRed staining. Standard curves and no-template controls were included in each reaction. The reactions for all the samples and standards were carried out in triplicate. The qPCR amplification reactions and thermal programs for all the studied genes are presented in Table S5 and Table S6, respectively. The number of targets per sample was calculated using Bio-Rad CFX Manager interface software. The amplification efficiencies of standards and the reaction ranges are shown in Table S7. The copies of all the target genes in all the samples were within the linear dynamic range of the standard curves.

2.6. Statistical analyses

All the statistical analyses were performed in R (Version 4.1.2, https://www.r-project.org) using specific packages, mainly *vegan* (Oksanen et al., 2019), *phyloseq* (McMurdie and Holmes, 2013), and *microeco* (Liu et al., 2020). The normality and homogeneity of the data were checked with Shapiro-Wilkinson and Levene tests respectively prior to downstream statistical analyses. Principal coordinates analysis (PCoA) based on Bray Curtis distance was used to characterize microbial community variation along the peatland chronosequence. Permutational multivariate analysis of variance (PERMANOVA) was used to test the differences in microbial community composition among categories such as peatland age class and sampling time. Standard Mantel tests were conducted to examine the relationships between microbial dissimilarities from Bray–Curtis distances and net MeHg formation proxies (MeHg and %MeHg) represented by their Euclidean distances. Partial least squares path modeling (PLS-PM) was conducted using the *seminr* package (Ray et al., 2021) to build up the relationships between latent variables—peat soil properties (e.g. pH, C/N ratio and elemental concentrations), microbial community composition (PCoA 1) and net MeHg formation (MeHg and %MeHg) across the peatland chronosequence. The relative abundance of microbial communities at family level that were significantly correlated (Spearman, $p < 0.05$) with net MeHg formation proxies was also used to predict net MeHg formation by Random Forest analyses using the *randomForest* package (Liaw and Wiener, 2002), with the more important microorganisms having higher mean decrease Gini coefficients. While Hg methylators known to possess *hgcAB* gene pair can directly transform inorganic Hg to MeHg, non-Hg methylator can also directly or indirectly influence net MeHg formation by degrading MeHg, modulating Hg bioavailability, or controlling the activity of the actual methylating/demethylating populations through microbial interactions. Here we defined putative Hg and non-Hg methylators according to whether or not they are known to carry methylation gene *hgcA* as inferred from a reference database compiled by Christensen et al. (2019). Co-occurrence networks were also established to determine underlying interactions between microbial taxa (at family level), including both the putative Hg methylators and other lineages without such traits. These networks were based on significant and strong correlations between microbial taxa (pairwise Spearman's rank correlations, $\rho > 0.40$ and $p < 0.01$). Only the taxa that were significantly ($p < 0.05$, Spearman) correlated with either MeHg or %MeHg were kept to relate the network to net MeHg formation along the peatland chronosequence. The networks were visualized using the interactive platform Gephi (Bastian et al., 2009).

3. Results

3.1. Relating microbial community composition to net MeHg formation

For all samples studied, microbial α-diversity indices (i.e. Chao1 and InvSimpson, indicating richness as well as the combined richness and evenness of microbial communities, respectively) were correlated negatively with THg, but positively with both MeHg concentrations and %MeHg in peat soil along this peatland chronosequence (Fig. S2). The composition of microbial communities differed significantly between the three peatland age classes (i.e. young, intermediate and old peatlands), between sampling years (2016 and 2017), and between the two peat layers (0–5 and 5–10 cm), whereas only 0.9% and 3% of the total variance in microbial community composition could be explained by sampling year and peat layer, respectively (Fig. 1a, Table S8). Notably, VPR treatment had no significant effects on microbial community composition (Table S8). The samples from VPR subplots were therefore used as replicates in the downstream statistical analyses. Overall, there were significant correlations between the microbial community composition and net MeHg formation proxies, MeHg ($r = 0.146$, $p < 0.0001$) and %MeHg ($r = 0.225$, $p < 0.0001$) along the peatland chronosequence (Mantel test, Fig. S3). The dissimilarity of microbial community composition indicated by PCoA 1 was also correlated positively with both MeHg and %MeHg, and explained 28% and 37% of the variance in MeHg and %MeHg, respectively (Fig. 1b, c). The PLS-PM analysis also showed similar results in that net MeHg formation proxies strongly correlated with the microbial community composition. These community features were also strongly correlated with soil properties, represented by pH, C/N as well as total concentrations of S, P, Fe, Mg, Mn, Zn and Ca (Fig. 2).

3.2. Key microbial taxa as predictors of net MeHg formation

The majority of the sequences of the peat samples studied were affiliated with a set of 58 families, where 14 families are known to harbor putative Hg methylators, mainly affiliated with *Deltaproteobacteria*, methanogenic *Archaea*, *Firmicutes*, *Chloroflexi*, *Spirochaetes* and *Ignavibacteriae*. Bacterial and archaeal families, such as *Spirochaetaceae*, *Anaerolineaceae*, *Opitutaceae*, *Syntrophaceae*, *Ignavibacteriaceae*, *Methanobacteriaceae*, *Methanoregulaceae*, *Methanotrichaceae*, *Geobacteraceae*, *Gallionellaceae*, *Desulfovibrionaceae* and some others, were those families most positively and strongly correlated with net MeHg formation proxies, MeHg concentration and %MeHg in peat soil. The families with strong negative correlations with net MeHg formation proxies included *Thermomonosporaceae*, *Planctomycetaceae*, *Methylocystaceae* and *Beijerinckiaceae* (Fig. S4). The Random Forest analyses showed similar results that the most influential guilds explaining net MeHg formation along the peatland chronosequence were canonical fermenters such as *Spirochaetaceae*, *Opitutaceae*, *Anaerolineaceae*, *Ignavibacteriaceae* and *Syntrophaceae*, followed by the lineages unlikely to be capable of MeHg formation (e.g. *Planctomycetaceae*, *Methylocystaceae* and *Thermomonosporaceae*) and a few known Hg methylating representatives, such as *Geobacteraceae* (FeRB), *Clostridiaceae_1* (Firmicutes) and *Methanoregulaceae* (methanogen). *Desulfovibrionaceae* is a family with well-known putative SRB Hg methylators, but appeared to be less important for net MeHg formation as compared to the families mentioned above (Fig. 3).

3.3. Co-occurrence of putative Hg and non-Hg methylators

In the correlation networks, there were 34 families (10 putative Hg methylators and 24 non-Hg methylators) with strong (pairwise Spearman's rank correlations, $\rho > 0.40$ and $p < 0.05$) co-occurrence patterns in the peat soils along the peatland chronosequence. A total of 5 modules were clearly clustered, with modules 1, 2, 3 and 5 having both putative Hg methylators and non-Hg methylators, while module 4 was altogether missing the lineages with known Hg methylating capacity (Fig. 4). Module 1 featured a higher diversity of putative Hg methylators compared to other modules with putative Hg methylators. Potential interactions were observed between Hg methylators (e.g. *Spirochaetaceae*, *Geobacteraceae* and *Anaerolineaceae*) as well as between Hg and non-Hg methylators (e.g. between *Spirochaetaceae* and *Planctomycetaceae*) (Fig. 4b).

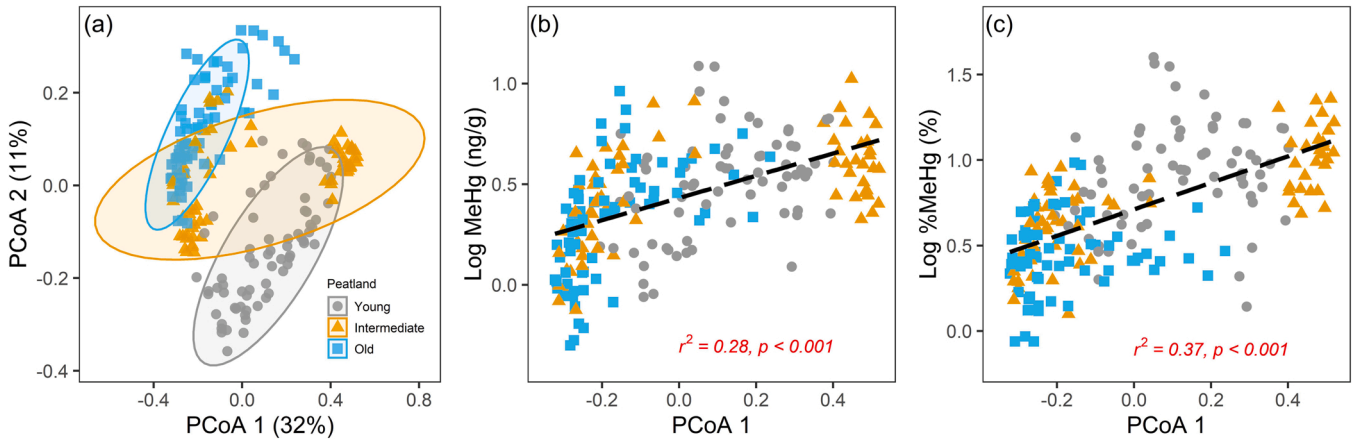

Fig. 1. Relationships between microbial community composition and net MeHg formation along the chronosequence of three peatland age classes. (a) Principal coordinates analysis (PCoA) characterizing microbial community composition along the peatland chronosequence. Correlations of microbial community represented by PCoA 1 with (b) MeHg concentrations and (c) %MeHg along the peatland chronosequence.

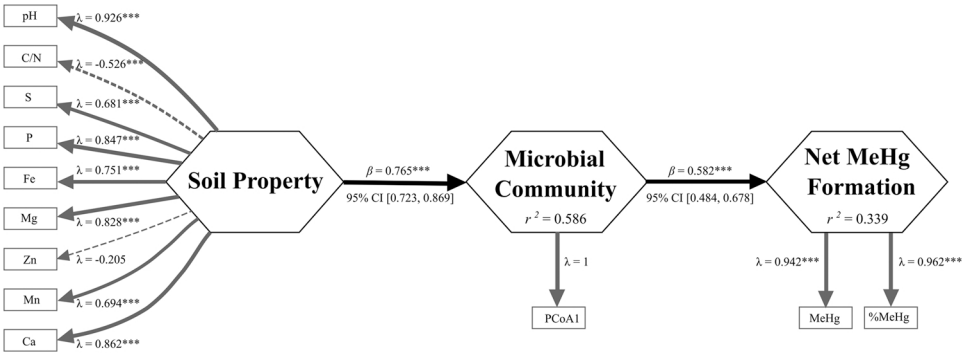

Fig. 2. Partial least squares path modeling (PLS-PM) demonstrating the associations between peat soil property (e.g. pH, C/N ratio and elemental concentrations), microbial community (PCoA 1) and net MeHg formation (MeHg and %MeHg) along the peatland chronosequence. Only the 90 samples that were measured for the concentrations of elements in the peat collected in 2016 were used for PLS-PM analyses. The λ coefficients are loadings calculated as correlations between a latent variable and its indicators, with asterisks indicating a significant difference (* $p < 0.05$, ** $p < 0.01$, *** $p < 0.001$). The β coefficients represent the path coefficients between microbial community and soil property as well as net MeHg formation. The thickness of the arrows filled in grey and black represents coefficients λ and β, respectively. The PLS-PM was bootstrapped 1000 times to obtain the 95% confidence intervals of the β path coefficients. The r^2 indicates the proportion of variance explained.

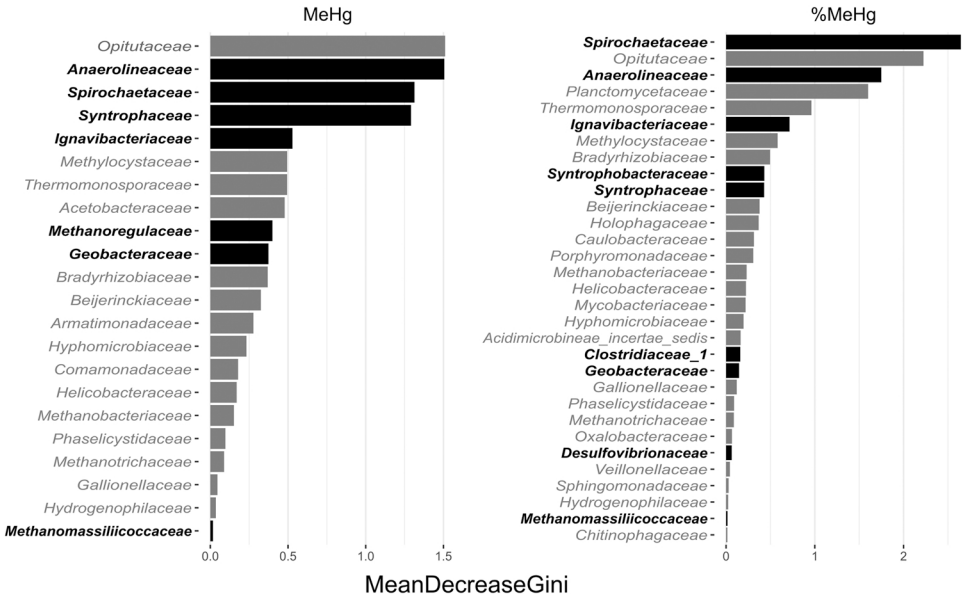

Fig. 3. Random forest analyses determining the importance of significant microbes at family level on net MeHg formation along the peatland chronosequence. Random forest analyses were carried out with 1000 trees and the mean decrease Gini coefficients were calculated from a set of 30 bootstrap samples. The more important a microbe is for net MeHg formation, the higher mean decrease Gini coefficient it has. The families in bold denote potential Hg methylators, while those in grey are non-Hg methylators.

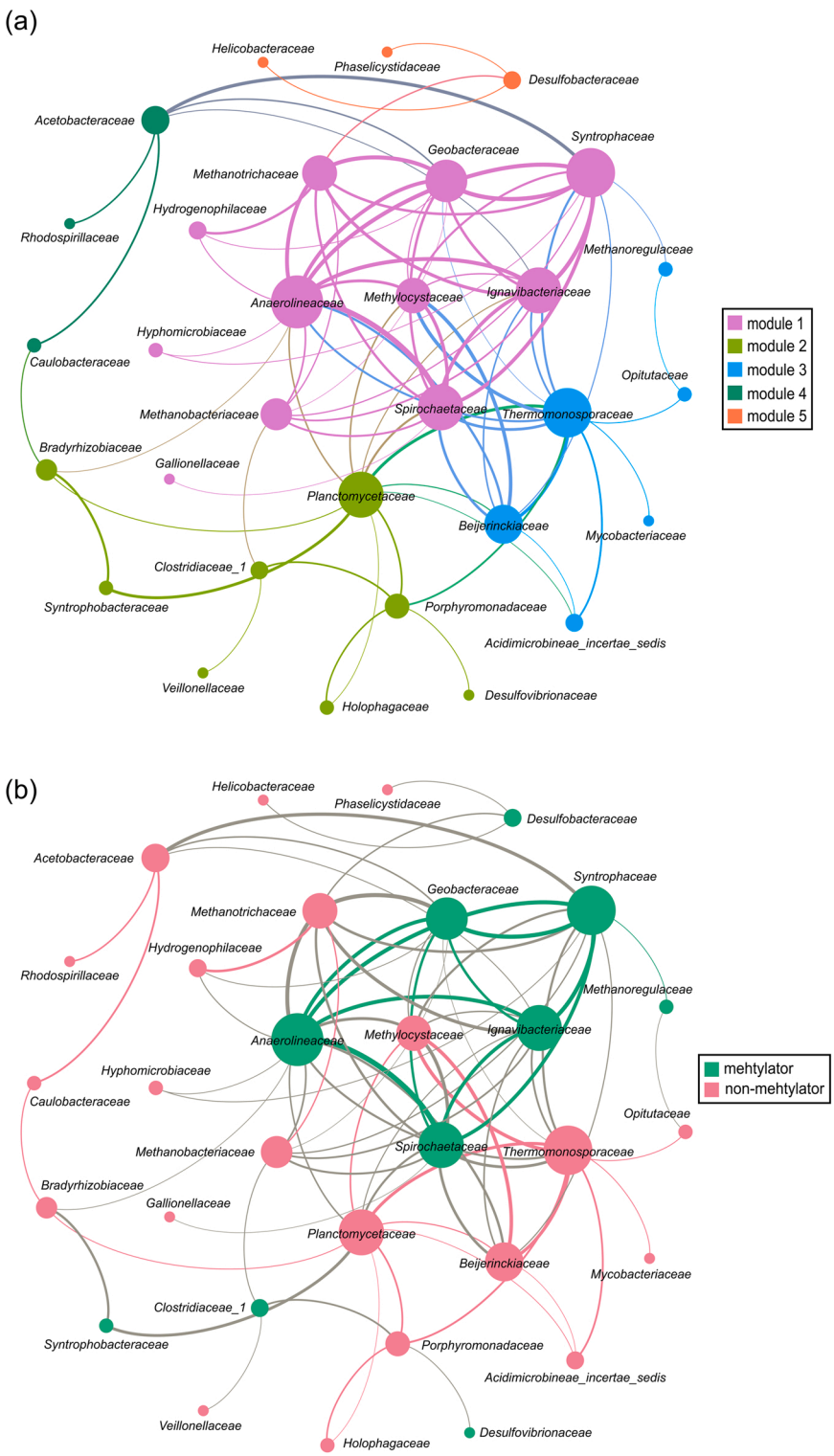

Fig. 4. The co-occurrence patterns of microbial communities relating to net MeHg formation along the peatland chronosequence. Those communities at family level that were significantly (Spearman) correlated with either MeHg or %MeHg were kept and represented by (a) 5 modules or (b) Hg and non-Hg methylators. The node size indicates the degree to which a node is connected by other nodes. The edges connecting nodes demonstrate strong ($\rho > 0.40$) and significant ($p < 0.01$) correlations between nodes, with the width of an edge representing correlation strength.

3.4. Comparisons of expressed marker genes and net MeHg formation

The expression of specific marker genes was quantified in this study with real time qPCR. While expressed *hgcA* transcripts from both Deltaproteobacteria and SRB-firmicutes were below detection, most genes could be quantified with 16S rRNA, *mcrA* and Archaea-*hgcA* transcripts all being significantly higher than *dsrA* transcripts. The transcripts did not differ between the three peatland age classes for any of the detected genes, except for *dsrA* transcripts which were significantly higher in the young peatlands as compared to the old (Fig. S5). The transcripts from 16S rRNA, *mcrA* and Archaea-*hgcA* genes were all positively correlated with both net MeHg formation proxies (MeHg concentration and % MeHg), with the sole exception that there was no significant correlation between *mcrA* transcripts and %MeHg. The *dsrA* transcripts did not correlate with either of the two proxies (Fig. 5).

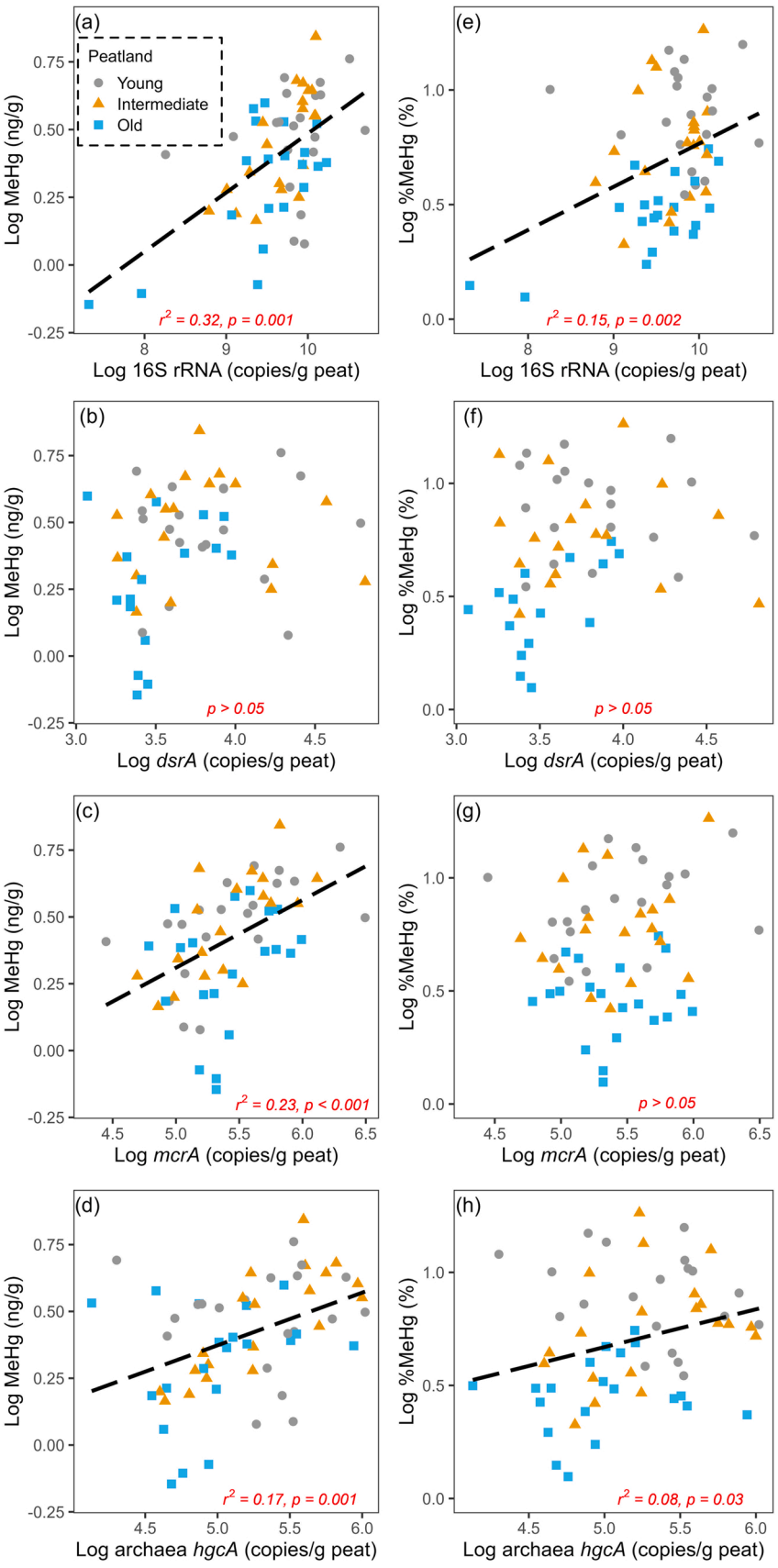

Fig. 5. Relationships between the abundance of specific gene transcript and MeHg concentration (left panels) and %MeHg (right panels) in peat along the peatland chronosequence. Significant correlations are indicated by dashed lines. The 60 combined samples of 0–5 and 5–10 cm peat layers collected from both control and vascular plant removal subplots in 2017 were used.

4. Discussion

4.1. Microbial community composition as a predictor of net MeHg formation along the peatland chronosequence

Net MeHg formation is largely the net effect of IHg methylation and MeHg demethylation in natural ecosystems, with microorganisms playing critical roles in both of the counteractive processes. Along the peatland chronosequence, significant differences in microbial community composition were observed between the three peatland age classes (Fig. 1a, Table S8). We hypothesize that changes in microbial community composition might be a critical factor determining net MeHg formation proxies (i.e. MeHg concentration and %MeHg in peat soil) that decline with peatland age along the peatland chronosequence (Hu et al., 2020; Wang et al., 2020, 2021). The diversity (i.e. alpha diversity indices) and composition (i.e. PCoA 1 and Bray-Curtis distances) of microbial community were all strongly associated with both of the two net MeHg formation proxies (Fig. S2, Fig. 1, Fig. S3). This finding is in agreement with analogous studies in rice paddies where the composition of microbial communities was tightly linked to MeHg concentration and %MeHg (Liu et al., 2019), but also contrasts with some earlier reports of insignificant or weak correlations between exclusive Hg methylating microorganisms and either MeHg concentration or Hg methylation rates (Christensen et al., 2019; Liu et al., 2019; Xu et al., 2021). Moreover, although there was no significant difference in 16S rRNA expression between the peatland age classes (Fig. S5), positive correlations were observed between 16S rRNA expression and the two net MeHg formation proxies (Fig. 5a, b). This suggests an important role of overall microbial activity beyond the activity of exclusive Hg methylating populations for predicting net MeHg formation.

It is known that peatland microbial communities are shaped by a wide range of environmental factors, such as pH and nutrient availability (Juottonen et al., 2005; Morales et al., 2006; Urbanová and Bárta, 2014). Accordingly, such environmentally controlled changes in the composition of microbial communities, including non-Hg and Hg methylating microorganisms, would likely result in variable net MeHg formation (Liu et al., 2019; Roth et al., 2021; Xu et al., 2021; Zhou et al., 2020). In agreement with this, our results showed a strong association between peat soil characteristics and microbial community composition and subsequently an indirect effect of peat soil characteristics on net MeHg formation (Fig. 2, Table S9). Moreover, redox variation induced by water regime can also influence Hg speciation and mobilization and consequently Hg bioavailability, resulting in a direct effect on MeHg formation (Beckers et al., 2019; Beckers and Rinklebe, 2017; Frohne et al., 2012; Jonsson et al., 2014; Zhu et al., 2018). Hence it is not surprising that previously reported correlations between peat soil characteristics and net MeHg formation along the chronosequence (Wang et al., 2020, 2021) may be explained by peat-soil control of microbial community composition or some type of interplay (Fig. 2, Table S9).

Interestingly, there were weak or insignificant effects of sampling year (wet in 2016 and dry in 2017) and month (June and August, representing spring and summer seasons), as well as peat layer (0–5 and 5–10 cm) and VPR treatment (vascular plant removal to reduce root exudates) on microbial community composition (Table S8). This may be because these boreal peatlands have similar high water saturation and DOC concentration along the year as well as similar soil temperature, largely independent of sampling time and VPR treatment, leading to a stable/resilient microbial community (Allison and Martiny, 2008). The weak or insignificant effects of these factors on microbial community composition may therefore explain their insignificant effects on net MeHg formation observed by our earlier studies along the peatland chronosequence (Wang et al., 2020, 2021).

4.2. Importance of the key taxa from both non-Hg and Hg methylators for net MeHg formation

Microorganisms in complex natural communities interact extensively with each other to obtain metabolic substrates and energy for growth and reproduction. Indeed, five highly interactive modules were also identified from the network of microbial communities along the chronosequence (Fig. 4a). The relative abundance of some fermentative, syntrophic, methanogenic, iron-reducing and nitrate-respiratory guilds and Archaea-*hgcA* transcripts (i.e. active methylating archaea) were all positively correlated with both MeHg concentration and %MeHg (Fig. S4, Fig. 5d, h). This suggests a direct or indirect role for those microbial guilds in the formation of MeHg. Indeed, fermentative, syntrophic, methanogenic and iron-reducing microorganisms have previously been associated with Hg methylation in boreal wetlands (Roth et al., 2021; Schaefer et al., 2020, 2014; Xu et al., 2021). It is noteworthy that the abundance of some methanogenic archaea (e.g. *Methanobacteriaceae* and *Methanoregulaceae*), which should in principle not be amplified with the primers used in this current study, were positively correlated with net MeHg formation (Fig. S4). Together with the relatively high *mcrA* and Archaea-*hgcA* transcripts (targeting active methanogens and Hg methylating archaea, respectively, Fig S6), these results suggest an underappreciated role of methanogens in net MeHg formation along the peatland chronosequence, likely by acting as Hg methylators in low-sulfate environments such as freshwater lakes and wetlands (Hamelin et al., 2011; Xu et al., 2021), syntrophic partners with methylating fermenters (Yu et al., 2018), or MeHg demethylators in rice paddies (Wu et al., 2020).

SRB are known to be efficient and prominent Hg methylators, but in this study, the relative abundance of SRB (e.g. *Desulfovibrionaceae*) and *dsrA* gene transcripts were all insignificantly or weakly correlated with MeHg concentrations or %MeHg (Fig. S4, Fig. 5). This may be because SRB include both Hg and non-Hg methylators. Some of these SRB (e.g. *Syntrophaceae*) which are putative Hg methylators can, instead of reducing sulfate, methylate Hg syntrophically with methanogens when sulfate is in short supply (McInerney et al., 2008; Pak and Bartha, 1998; Schaefer et al., 2020; Yu et al., 2010). This is further supported by our previous findings that SRB, likely those metabolizing alternative substrates instead of sulfate, are responsible for Hg methylation along the peatland chronosequence, as evidenced by the inhibitory effects of molybdate addition and the insignificant or inhibitory effects of sulfate amendment on Hg methylation in laboratory incubations (Hu et al., 2020). Furthermore, the low abundance of transcripts from *dsrA* relative to expressed Archaea-*hgcA* (Fig. S5) suggests a less significant role of SRB in net MeHg formation along the peatland chronosequence, as compared to other studied ecosystems showing a dominant role of SRB in MeHg formation (Compeau and Bartha, 1985; Gilmour et al., 1992, 2013).

Notably, Deltaproteobacteria-*hgcA* and SRB-firmicutes-*hgcA* transcripts could not be detected by qPCR in the peat soils along the chronosequence. This was not because of loss of mRNA or presence of inhibitory substances but likely as a result of primer bias or low abundance of these clades, as other relevant gene transcripts, including *mcrA*, *dsrA* and Archaea-*hgcA*, were robustly detected (Fig S5). Additionally, caution should also be exercised when inferring capacity for Hg methylation based on 16S rRNA data. Lineages previously identified as Hg methylators can also include strains that lack this capacity (Bridou et al., 2011; Gilmour et al., 2011). Increased use of *hgcA* gene-related detection methods, such as *hgcA* gene sequencing, genome-resolved metagenomics and metatranscriptomics, are identifying novel putative methylators in other taxa besides the previously recognized *Deltaproteobacteria*, *Firmicutes* and methanogenic archaea. These novel methylators as identified by other studies are affiliated with a broad range of taxa including *Chlorofexi*, *Nitrospirota*, *Spirochaetes*, *Actinobacteria*, *Planctomycetes* and *Verrucomicrobia* (McDaniel et al., 2020; Peterson et al., 2020; Xu et al., 2019, 2021), none of which have previously been

thought of as being Hg methylators.

Although microbial Hg methylation is the main source of MeHg in natural ecosystems, this process does not depend on a single methylating guild but rather complex metabolic interactions among microorganisms (Bravo et al., 2018a; Correia et al., 2012). This is further corroborated by our observed interactions both among putative Hg methylators as well as between such populations and non-Hg methylators (Fig. 4b). The MeHg concentration and %MeHg were also significantly correlated with both putative non-Hg and Hg methylators, suggesting that both can be important for net MeHg formation in the peatlands (Fig. S4, Fig. 3). For example, members of the *Opitutaceae* (e.g. the type species *Opitutus terrae*, a putative non-Hg methylator) are fermenters that can produce a variety of organic acids such as propionate, lactate and acetate. These can eventually serve as important substrates for methanogens (Rodrigues and Isanapong, 2014) that are a group known to engage in Hg methylation in natural ecosystems (Hamelin et al., 2011; Wood et al., 1968).

Moreover, the relative abundance of some methanotrophs (e.g. *Methylocystaceae* and *Beijerinckiaceae*) were negatively correlated with the two net MeHg formation proxies (Fig. S4). This can be explained by the involvement of methanotrophs (e.g. *Methylosinus trichosporium* OB3b) in the degradation of MeHg, likely by means of an initial binding to methanobactin (Barkay and Gu, 2022; Lu et al., 2017). Some other non-Hg methylating microbial taxa, such as *Catenulisporaceae*, *Frankiaceae*, *Mycobacteriaceae* and *Thermomonosporaceae*, have also been suggested by metatranscriptomic analyses to directly or indirectly influence MeHg degradation in rice paddies (Zhou et al., 2020). In line with this, negative correlations were shown between the relative abundance of *Thermomonosporaceae* and the two net MeHg formation proxies (Fig. S4). All of these results suggest that diverse microbial guilds are mediating MeHg demethylation that may in return directly control net MeHg formation in these peatlands. However, more work is needed to disentangle processes and organisms responsible for MeHg degradation along the peatland chronosequence.

5. Conclusions

Our study aimed to assess whether the composition of microbial communities, including both non-Hg and Hg methylating microorganisms, could explain net MeHg formation along a trophic gradient in a peatland chronosequence. The composition and activity of total microbial communities, including both putative Hg and non-Hg methylators, were significantly associated with the two net MeHg formation proxies, MeHg concentration and %MeHg in peat soil along the peatland chronosequence. While potential Hg methylators (e.g. some fermentative, syntrophic, methanogenic, iron-reducing and nitrate-respiratory metabolic guilds) could directly influence Hg methylation, non-Hg methylators also seemed to play an important role in net MeHg formation. The influence of the non-Hg methylators is presumably exerted by modulating the bioavailability of Hg for use in methylating/demethylating processes, and/or by controlling the activity of the actual methylating/demethylating populations through competition or other microbial interactions, and/or by reducing MeHg via direct demethylation. The SRB, known as efficient and prominent Hg methylators, appeared to play a less significant role in net MeHg formation along the peatland chronosequence as compared to other studied ecosystems. The involvement of both Hg and non-Hg methylating microorganisms in predicting net MeHg formation along the peatland chronosequence highlights the relevance of studying the entire microbial community in natural habitats for a better understanding of net MeHg formation.

Environmental Implication

Methylmercury (MeHg) is highly toxic to wildlife and humans because it can bioaccumulate and biomagnify in food webs. Net MeHg formation is not only dependent on Hg methylating microbes but the entire communities where Hg methylators are embedded. This work is a novel determination of the role of the entire microbial community, including Hg and non-Hg methylators, on net MeHg formation along a peatland chronosequence trophic gradient that has similar atmospheric deposition, climate patterns and underlying geology. It highlights the relevance of studying the entire microbial community in natural habitats for a better understanding of net MeHg formation.

CRediT authorship contribution statement

Baolin Wang: Writing – original draft, Visualization, Investigation, Conceptualization. **Haiyan Hu**: Writing – review & editing, Conceptualization. **Kevin Bishop**: Writing – review & editing, Funding acquisition, Conceptualization. **Moritz Buck**: Bioinformatical analysis. **Erik Björn**: Writing – review & editing, Methodology. **Ulf Skyllberg**: Writing – review & editing, Methodology, Conceptualization. **Mats B. Nilsson**: Writing – review & editing, Methodology, Conceptualization. **Stefan Bertilsson**: Writing – review & editing, Methodology, Conceptualization. **Andrea G. Bravo**: Writing – review & editing, Methodology, Conceptualization.

Declaration of Competing Interest

The authors declare that they have no known competing financial interests or personal relationships that could have appeared to influence the work reported in this paper.

Data Availability

Data will be made available on request.

Acknowledgments

We would like to thank Tao Jiang, Liem Nguyen, Yu Song and Wei Zhu for their great help in the laboratory, and Lucas Perreal, Camille Guyenot, Thibaut Imbert, Edward van Westrene, Marloes Arens, Mélissa Garsany, Laura Manteau, Jeanne Latour, Charles Sanseverino, Quan Zhou and Itziar Aguinaga Gil for the sampling. We acknowledge the UPPMAX platform (Uppsala Multidisciplinary Center for Advanced Computational Science) at Uppsala University (https://www.uppmax.uu.se) for computational and data storage resources. This work was supported by the National Natural Science Foundation of China (No. 42177114, 41931297 and 41573078), the China Scholarship Council (CSC; No. 201408520034), the Guizhou Provincial Science and Technology Projects (ZK[2022]568), the Swedish Research Council (VR2013–6978), and the Swedish Research Council Formas (2016–00896).

Appendix A. Supporting information

Supplementary data associated with this article can be found in the online version at doi:10.1016/j.jhazmat.2022.130057.

References

Åkerblom, S., Nilsson, M.B., Skyllberg, U., Björn, E., Jonsson, S., Ranneby, B., Bishop, K., 2020. Formation and mobilization of methylmercury across natural and experimental sulfur deposition gradients. Environ. Pollut. 263, 114398.

Allison, S.D., Martiny, J.B.H., 2008. Resistance, resilience, and redundancy in microbial communities. Proc. Natl. Acad. Sci. 105, 11512–11519.

Barkay, T., Gu, B., 2022. Demethylation—The Other Side of the Mercury Methylation Coin: A Critical Review. ACS Environ. Au 2, 77–97.

Barkay, T., Wagner-Döbler, I., 2005. Microbial Transformations of Mercury: Potentials, Challenges, and Achievements in Controlling Mercury Toxicity in the Environment. Advances in Applied Microbiology. Academic Press,, pp. 1–52.

Bastian M., Heymann S. and Jacomy M. (2009) Gephi: An Open Source Software for Exploring and Manipulating Networks. Proceedings of the International AAAI Conference on Web and Social Media **3**, 361–362.

Beckers, F., Rinklebe, J., 2017. Cycling of mercury in the environment: Sources, fate, and human health implications: A review. Crit. Rev. Environ. Sci. Technol. 47, 693–794.
Beckers, F., Mothes, S., Abrigata, J., Zhao, J., Gao, Y., Rinklebe, J., 2019. Mobilization of mercury species under dynamic laboratory redox conditions in a contaminated floodplain soil as affected by biochar and sugar beet factory lime. Sci. Total Environ. 672, 604–617.
Bergman, I., Bishop, K., Tu, Q., Frech, W., Akerblom, S., Nilsson, M., 2012. The Influence of Sulphate Deposition on the Seasonal Variation of Peat Pore Water Methyl Hg in a Boreal Mire. Plos One 7, 10.
Bishop, K., Shanley, J.B., Riscassi, A., de Wit, H.A., Eklöf, K., Meng, B., Mitchell, C., Osterwalder, S., Schuster, P.F., Webster, J., Zhu, W., 2020. Recent advances in understanding and measurement of mercury in the environment: Terrestrial Hg cycling. Sci. Total Environ. 721, 137647.
Bouchet, S., Goñi-Urriza, M., Monperrus, M., Guyoneaud, R., Fernandez, P., Heredia, C., Tessier, E., Gassie, C., Point, D., Guédron, S., Achá, D., Amouroux, D., 2018. Linking Microbial Activities and Low-Molecular-Weight Thiols to Hg Methylation in Biofilms and Periphyton from High-Altitude Tropical Lakes in the Bolivian Altiplano. Environ. Sci. Technol. 52, 9758–9767.
Bragazza, L., Bardgett, R.D., Mitchell, E.A.D., Buttler, A., 2015. Linking soil microbial communities to vascular plant abundance along a climate gradient. N. Phytol. 205, 1175–1182.
Bravo, A.G., Loizeau, J.-L., Dranguet, P., Makri, S., Björn, E., Ungureanu, V.G., Slaveykova, V.I., Cosio, C., 2016. Persistent Hg contamination and occurrence of Hg-methylating transcript (hgcA) downstream of a chlor-alkali plant in the Olt River (Romania). Environ. Sci. Pollut. Res. 23, 10529–10541.
Bravo, A.G., Peura, S., Buck, M., Ahmed, O., Mateos-Rivera, A., Herrero Ortega, S., Schaefer, J.K., Bouchet, S., Tolu, J., Bjorn, E., Bertilsson, S., 2018a. Methanogens and Iron-Reducing Bacteria: the Overlooked Members of Mercury-Methylating Microbial Communities in Boreal Lakes. Appl. Environ. Microbiol **84**.
Bravo, A.G., Zopfi, J., Buck, M., Xu, J., Bertilsson, S., Schaefer, J.K., Poté, J., Cosio, C., 2018b. Geobacteraceae are important members of mercury-methylating microbial communities of sediments impacted by waste water releases. ISME J. 12, 802–812.
Bridou, R., Monperrus, M., Gonzalez, P.R., Guyoneaud, R., Amouroux, D., 2011. Simultaneous determination of mercury methylation and demethylation capacities of various sulfate-reducing bacteria using species-specific isotopic tracers. Environ. Toxicol. Chem. 30, 337–344.
Christensen, G.A., Gionfriddo, C.M., King, A.J., Moberly, J.G., Miller, C.L., Somenahally, A.C., Callister, S.J., Brewer, H., Podar, M., Brown, S.D., Palumbo, A.V., Brandt, C.C., Wymore, A.M., Brooks, S.C., Hwang, C., Fields, M.W., Wall, J.D., Gilmour, C.C., Elias, D.A., 2019. Determining the Reliability of Measuring Mercury Cycling Gene Abundance with Correlations with Mercury and Methylmercury Concentrations. Environ. Sci. Technol. 53, 8649–8663.
Clarkson, T.W., Magos, L., 2006. The Toxicology of Mercury and Its Chemical Compounds. Crit. Rev. Toxicol. 36, 609–662.
Cole, J.R., Wang, Q., Fish, J.A., Chai, B., McGarrell, D.M., Sun, Y., Brown, C.T., Porras-Alfaro, A., Kuske, C.R., Tiedje, J.M., 2013. Ribosomal Database Project: data and tools for high throughput rRNA analysis. Nucleic Acids Res. 42, D633–D642.
Compeau, G.C., Bartha, R., 1985. Sulfate-Reducing Bacteria: Principal Methylators of Mercury in Anoxic Estuarine Sediment. Appl. Environ. Microbiol. 50, 498–502.
Correia, R.R.S., Miranda, M.R., Guimarães, J.R.D., 2012. Mercury methylation and the microbial consortium in periphyton of tropical macrophytes: Effect of different inhibitors. Environ. Res. 112, 86–91.
Drott, A., Lambertsson, L., Björn, E., Skyllberg, U., 2008. Do Potential Methylation Rates Reflect Accumulated Methyl Mercury in Contaminated Sediments? Environ. Sci. Technol. 42, 153–158.
Edgar, R.C., 2010. Search and clustering orders of magnitude faster than BLAST. Bioinformatics 26, 2460–2461.
Edgar, R.C., 2016. SINTAX: a simple non-Bayesian taxonomy classifier for 16S and ITS sequences. bioRxiv, 074161.
Feng, X., Li, P., Qiu, G., Wang, S., Li, G., Shang, L., Meng, B., Jiang, H., Bai, W., Li, Z., Fu, X., 2008. Human Exposure To Methylmercury through Rice Intake in Mercury Mining Areas, Guizhou Province, China. Environ. Sci. Technol. 42, 326–332.
Fisk, M.C., Ruether, K.F., Yavitt, J.B., 2003. Microbial activity and functional composition among northern peatland ecosystems. Soil Biol. Biochem. 35, 591–602.
Fleming, E.J., Mack, E.E., Green, P.G., Nelson, D.C., 2006. Mercury methylation from unexpected sources: molybdate-inhibited freshwater sediments and an iron-reducing bacterium. Appl. Environ. Microbiol 72, 457–464.
Frohne, T., Rinklebe, J., Langer, U., Du Laing, G., Mothes, S., Wennrich, R., 2012. Biogeochemical factors affecting mercury methylation rate in two contaminated floodplain soils. Biogeosciences 9, 493–507.
Gilmour, C.C., Henry, E.A., Mitchell, R., 1992. Sulfate stimulation of mercury methylation in freshwater sediments. Environ. Sci. Technol. 26, 2281–2287.
Gilmour, C.C., Elias, D.A., Kucken, A.M., Brown, S.D., Palumbo, A.V., Schadt, C.W., Wall, J.D., 2011. Sulfate-reducing bacterium Desulfovibrio desulfuricans ND132 as a model for understanding bacterial mercury methylation. Appl. Environ. Microbiol 77, 3938–3951.
Gilmour, C.C., Podar, M., Bullock, A.L., Graham, A.M., Brown, S.D., Somenahally, A.C., Johs, A., Hurt, R.A., Bailey, K.L., Elias, D.A., 2013. Mercury Methylation by Novel Microorganisms from New Environments. Environ. Sci. Technol. 47, 11810–11820.
Grégoire, D.S., Poulain, A.J., 2018. Shining light on recent advances in microbial mercury cycling. FACETS 3, 858–879.
Hamelin, S., Amyot, M., Barkay, T., Wang, Y., Planas, D., 2011. Methanogens: principal methylators of mercury in lake periphyton. Environ. Sci. Technol. 45, 7693–7700.
Haynes, K.M., Kane, E.S., Potvin, L., Lilleskov, E.A., Kolka, R.K., Mitchell, C.P.J., 2017. Mobility and transport of mercury and methylmercury in peat as a function of changes in water table regime and plant functional groups. Glob. Biogeochem. Cycles 31, 233–244.
Hong, Y.-S., Kim, Y.-M., Lee, K.-E., 2012. Methylmercury exposure and health effects. J. Prev. Med Public Health 45, 353–363.
Hu, H., Wang, B., Bravo, A.G., Björn, E., Skyllberg, U., Amouroux, D., Tessier, E., Zopfi, J., Feng, X., Bishop, K., Nilsson, M.B., Bertilsson, S., 2020. Shifts in mercury methylation across a peatland chronosequence: From sulfate reduction to methanogenesis and syntrophy. J. Hazard. Mater. 387, 121967.
Hünicke, B., Zorita, E., Soomere, T., Madsen, K.S., Johansson, M., Suursaar, Ü., 2015. Recent Change—Sea Level and Wind Waves. In: The, B.I.I.A.T. (Ed.), Second Assessment of Climate Change for the Baltic Sea Basin. Springer International Publishing, Cham, pp. 155–185.
Jonsson, S., Skyllberg, U., Nilsson, M.B., Lundberg, E., Andersson, A., Björn, E., 2014. Differentiated availability of geochemical mercury pools controls methylmercury levels in estuarine sediment and biota. Nat. Commun. 5, 4624.
Juottonen, H., Galand, P.E., Tuittila, E.-S., Laine, J., Fritze, H., Yrjälä, K., 2005. Methanogen communities and Bacteria along an ecohydrological gradient in a northern raised bog complex. Environ. Microbiol. 7, 1547–1557.
Kerin, E.J., Gilmour, C.C., Roden, E., Suzuki, M.T., Coates, J.D., Mason, R.P., 2006. Mercury Methylation by Dissimilatory Iron-Reducing Bacteria. Appl. Environ. Microbiol. 72, 7919–7921.
Lambertsson, L., Lundberg, E., Nilsson, M., Frech, W., 2001. Applications of enriched stable isotope tracers in combination with isotope dilution GC-ICP-MS to study mercury species transformation in sea sediments during in situ ethylation and determination. J. Anal. At. Spectrom. 16, 1296–1301.
Liaw, A., Wiener, M.C., 2002. Classification and Regression by randomForest. R. N. 2, 18–22.
Liu, C., Cui, Y., Li, X., Yao, M., 2020. microeco: an R package for data mining in microbial community ecology. FEMS Microbiol. Ecol. **97**.
Liu, Y.-R., Johs, A., Bi, L., Lu, X., Hu, H.-W., Sun, D., He, J.-Z., Gu, B., 2018. Unraveling Microbial Communities Associated with Methylmercury Production in Paddy Soils. Environ. Sci. Technol. 52, 13110–13118.
Liu, Y.-R., Yang, Z., Zhou, X., Qu, X., Li, Z., Zhong, H., 2019. Overlooked Role of Putative Non-Hg Methylators in Predicting Methylmercury Production in Paddy Soils. Environ. Sci. Technol. 53, 12330–12338.
Lu, X., Gu, W.Y., Zhao, L.D., Farhan Ul Haque, M., DiSpirito, A.A., Semrau, J.D., Gu, B.H., 2017. Methylmercury uptake and degradation by methanotrophs. Sci. Adv. **3**.
McDaniel, E.A., Peterson, B.D., Stevens, S.L.R., Tran, P.Q., Anantharaman, K., McMahon, K.D., 2020. Expanded Phylogenetic Diversity and Metabolic Flexibility of Mercury-Methylating Microorganisms. mSystems **5**.
McInerney, M.J., Struchtemeyer, C.G., Sieber, J., Mouttaki, H., Stams, A.J.M., Schink, B., Rohlin, L., Gunsalus, R.P., 2008. Physiology, Ecology, Phylogeny, and Genomics of Microorganisms Capable of Syntrophic Metabolism. Ann. Ny. Acad. Sci. 1125, 58–72.
McMurdie, P.J., Holmes, S., 2013. phyloseq: An R Package for Reproducible Interactive Analysis and Graphics of Microbiome Census Data. PLOS ONE 8, e61217.
Meng, B., Feng, X.B., Qiu, G.L., Liang, P., Li, P., Chen, C.X., Shang, L.H., 2011.) The Process of Methylmercury Accumulation in Rice (Oryza sativa L.). Environ. Sci. Technol. 45, 2711–2717.
Mitchell, C.P.J., Branfireun, B.A., Kolka, R.K., 2008. Spatial Characteristics of Net Methylmercury Production Hot Spots in Peatlands. Environ. Sci. Technol. 42, 1010–1016.
Morales, S.E., Mouser, P.J., Ward, N., Hudman, S.P., Gotelli, N.J., Ross, D.S., Lewis, T.A., 2006. Comparison of Bacterial Communities in New England Sphagnum Bogs Using Terminal Restriction Fragment Length Polymorphism (T-RFLP). Microb. Ecol. 52, 34–44.
Oksanen, J., Blanchet, F.G., Friendly, M., Kindt, R., Legendre, P., McGlinn, D., Minchin, P.R., 2019. vegan: Community Ecology Package, R package version. 5-6 ed 2.
Pak, K., Bartha, R., 1998. Mercury methylation by interspecies hydrogen and acetate transfer between sulfidogens and methanogens. Appl. Environ. Microbiol. 64, 1987–1990.
Paranjape, A.R., Hall, B.D., 2017. Recent advances in the study of mercury methylation in aquatic systems. FACETS 2, 85–119.
Peterson, B.D., McDaniel, E.A., Schmidt, A.G., Lepak, R.F., Janssen, S.E., Tran, P.Q., Marick, R.A., Ogorek, J.M., DeWild, J.F., Krabbenhoft, D.P., McMahon, K.D., 2020. Mercury Methylation Genes Identified across Diverse Anaerobic Microbial Guilds in a Eutrophic Sulfate-Enriched Lake. Environ. Sci. Technol. 54, 15840–15851.
Podar, M., Gilmour, C.C., Brandt, C.C., Soren, A., Brown, S.D., Crable, B.R., Palumbo, A. V., Somenahally, A.C., Elias, D.A., 2015. Global prevalence and distribution of genes and microorganisms involved in mercury methylation. Sci. Adv. **1**.
Ray S., Danks N.P. and Valdez A.C. (2021) seminr: Building and Estimating Structural Equation Models, R package version 2.2.1 ed.
Rodrigues, J.L.M., Isanapong, J., 2014. The Family Opitutaceae. In: Rosenberg, E., DeLong, E.F., Lory, S., Stackebrandt, E., Thompson, F. (Eds.), The Prokaryotes: Other Major Lineages of Bacteria and The Archaea. Springer Berlin Heidelberg, Berlin, Heidelberg, pp. 751–756.
Rognes, T., Flouri, T., Nichols, B., Quince, C., Mahé, F., 2016. VSEARCH: a versatile open source tool for metagenomics. PeerJ 4, e2584.
Roth, S., Poulin, B.A., Baumann, Z., Liu, X., Zhang, L., Krabbenhoft, D.P., Hines, M.E., Schaefer, J.K., Barkay, T., 2021. Nutrient Inputs Stimulate Mercury Methylation by Syntrophs in a Subarctic Peatland. Front. Microbiol. **12**.
Schaefer, J.K., Kronberg, R.M., Morel, F.M.M., Skyllberg, U., 2014. Detection of a key Hg methylation gene, hgcA, in wetland soils. Environ. Microbiol. Rep. 6, 441–447.
Schaefer, J.K., Kronberg, R.-M., Björn, E., Skyllberg, U., 2020. Anaerobic guilds responsible for mercury methylation in boreal wetlands of varied trophic status

serving as either a methylmercury source or sink. Environ. Microbiol. 22, 3685–3699.
Sinclair, L., Osman, O.A., Bertilsson, S., Eiler, A., 2015. Microbial Community Composition and Diversity via 16S rRNA Gene Amplicons: Evaluating the Illumina Platform. PLOS ONE 10, e0116955.
St. Louis, V.L., Rudd, J.W.M., Kelly, C.A., Beaty, K.G., Flett, R.J., Roulet, N.T., 1996. Production and Loss of Methylmercury and Loss of Total Mercury from Boreal Forest Catchments Containing Different Types of Wetlands. Environ. Sci. Technol. 30, 2719–2729.
Tjerngren, I., Meili, M., Bjorn, E., Skyllberg, U., 2012. Eight Boreal Wetlands as Sources and Sinks for Methyl Mercury in Relation to Soil Acidity, C/N Ratio, and Small-Scale Flooding. Environ. Sci. Technol. 46, 8052–8060.
Urbanová, Z., Bárta, J., 2014. Microbial community composition and in silico predicted metabolic potential reflect biogeochemical gradients between distinct peatland types. FEMS Microbiol. Ecol. 90, 633–646.
Wang, B., Nilsson, M.B., Eklöf, K., Hu, H., Ehnvall, B., Bravo, A.G., Zhong, S., Åkeblom, S., Björn, E., Bertilsson, S., Skyllberg, U., Bishop, K., 2020. Opposing spatial trends in methylmercury and total mercury along a peatland chronosequence trophic gradient. Sci. Total Environ. 718, 137306.
Wang, B., Zhong, S., Bishop, K., Nilsson, M.B., Hu, H., Eklöf, K., Bravo, A.G., Åkerblom, S., Bertilsson, S., Björn, E., Skyllberg, U., 2021. Biogeochemical influences on net methylmercury formation proxies along a peatland chronosequence. Geochim. Et. Cosmochim. Acta 308, 188–203.
Wood, J.M., Kennedy, F.S., Rosen, C.G., 1968. Synthesis of methyl-mercury compounds by extracts of a methanogenic bacterium. Nature 220, 173–174.
Wu, Q., Hu, H., Meng, B., Wang, B., Poulain, A.J., Zhang, H., Liu, J., Bravo, A.G., Bishop, K., Bertilsson, S., Feng, X., 2020. Methanogenesis Is an Important Process in Controlling MeHg Concentration in Rice Paddy Soils Affected by Mining Activities. Environ. Sci. Technol. 54, 13517–13526.
Xu, J., Buck, M., Eklöf, K., Ahmed, O.O., Schaefer, J.K., Bishop, K., Skyllberg, U., Björn, E., Bertilsson, S., Bravo, A.G., 2019. Mercury methylating microbial communities of boreal forest soils. Sci. Rep. 9, 518.
Xu, J., Liem-Nguyen, V., Buck, M., Bertilsson, S., Björn, E., Bravo, A.G., 2021. Mercury Methylating Microbial Community Structure in Boreal Wetlands Explained by Local Physicochemical Conditions. Front. Environ. Sci. **8**.
Yu, R.-Q., Adatto, I., Montesdeoca, M.R., Driscoll, C.T., Hines, M.E., Barkay, T., 2010. Mercury methylation in Sphagnum moss mats and its association with sulfate-reducing bacteria in an acidic Adirondack forest lake wetland. FEMS Microbiol. Ecol. 74, 655–668.
Yu, R.-Q., Reinfelder, J.R., Hines, M.E., Barkay, T., 2018. Syntrophic pathways for microbial mercury methylation. ISME J. 12, 1826–1835.
Zhang, H., Feng, X., Larssen, T., Qiu, G., Vogt, R.D., 2010a. In Inland China, Rice, Rather than Fish, Is the Major Pathway for Methylmercury Exposure. Environ. Health Perspect. 118, 1183–1188.
Zhang, H., Feng, X.B., Larssen, T., Shang, L., Li, P., 2010b. Bioaccumulation of Methylmercury versus Inorganic Mercury in Rice (Oryza sativa L.) Grain. Environ. Sci. Technol. 44, 4499–4504.
Zhou, X.-Q., Hao, Y.-Y., Gu, B., Feng, J., Liu, Y.-R., Huang, Q., 2020. Microbial Communities Associated with Methylmercury Degradation in Paddy Soils. Environ. Sci. Technol. 54, 7952–7960.
Zhu, W., Song, Y., Adediran, G.A., Jiang, T., Reis, A.T., Pereira, E., Skyllberg, U., Björn, E., 2018. Mercury transformations in resuspended contaminated sediment controlled by redox conditions, chemical speciation and sources of organic matter. Geochim. Et. Cosmochim. Acta 220, 158–179.